Earth and Planetary Science Letters 298 (2010) 217–228

Contents lists available at ScienceDirect

Earth and Planetary Science Letters

journal homepage: www.elsevier.com/locate/epsl

Changes in Eastern Pacific ocean ventilation at intermediate depth over the last 150 kyr BP

G. Leduc *, L. Vidal, K. Tachikawa, E. Bard

CEREGE, Aix-Marseille Université; CNRS; Collège de France; IRD; Europôle Méditerranéen de L'Arbois, BP 80, 13545 Aix en Provence, France

ARTICLE INFO

Article history:
Received 24 June 2009
Received in revised form 31 July 2010
Accepted 3 August 2010

Editor: P. DeMenocal

Keywords:
Thermohaline Circulation
Pacific Ocean
last glacial period
benthic foraminifera
stable isotopes

ABSTRACT

The circulation patterns of the deep glacial Pacific Ocean are still debated. Difficulties arise due to the scarcity of reliable paleoceanographic records that can document the past movements and properties of Pacific Ocean water masses. Here, we jointly use $\delta^{13}C$ and $\delta^{18}O$ measured on the epibenthic foraminifer *Cibicidoides wuellerstorfi*, from the MD02-2529 sediment core collected at 1619 m water depth in the eastern equatorial Pacific, to monitor changes in water mass circulation spanning the past 150 kyr BP. After the extraction of short-term (centennial to millennial-scale) $\delta^{13}C$ and $\delta^{18}O$ changes, which were ~1.0 and 0.5‰, respectively, we observed that these rapid $\delta^{13}C$ and $\delta^{18}O$ shifts were closely interrelated during the last 150 kyr BP. A comparison of MD02-2529 with other benthic $\delta^{13}C$ records localized to the north and south of the core location revealed that MD02-2529 was alternately bathed by a northern nutrient-rich and a southern nutrient-poor water mass. The comparison provided a diagnostic for the latitudinal movements of a sharp water mass front that was particularly evident during marine isotope stages 4 and 3 on the millennial timescale. By considering that $\delta^{13}C$ is an indicator of the northern vs. southern origin of the water that bathed the MD02-2529 coring site in the past, we found that a North Pacific water mass, that occasionally spreads to the eastern Pacific Ocean as deep as 1600 m and as far south as 8°N, was responsible for shifts toward the positive $\delta^{18}O$ we observed in the past. We then used the $\delta^{13}C/\delta^{18}O$ relationship to reconstruct latitudinal temperature and/or salinity gradients of the water mass that were linked to changes in the northern and/or the southern water mass end-members. Evolution of the $\delta^{13}C/\delta^{18}O$ relationship spanning the past 150 kyr BP has shed light on how hydrological processes occurring at northern and southern high latitudes are transmitted to the ocean's interior through water mass advection.

1. Introduction

Modern deep-water formation sites are localized in the northern North Atlantic and around Antarctica in the Weddell and Ross Seas (Kuhlbrodt et al., 2007), while there is no deep-water formation in the North Pacific. North Atlantic Deep Water (NADW) ventilates most of the present-day deep Atlantic Ocean. The fact that there is no NADW equivalent for the North Pacific makes the present-day Thermohaline Circulation (THC) asymmetric. The absence of North Pacific deep-water formation leads to oxygen depletion between ~500 and ~2500 m in the entire present-day North Pacific Ocean (Helly and Levin, 2004) (Fig. 1a).

Drastic changes in Pacific Ocean circulation triggered by high-latitude hydrological processes are candidates for explaining part of the observed changes in atmospheric carbon dioxide during the Pleistocene (Haug and Sigman, 2009; Sigman et al., 2010). However, up until now there have not been any simple schemes for how past circulation in the Pacific could have differed from modern circulation. On one hand, an increase in the nutrient content of the deep glacial ocean could suggest that deep Pacific Ocean circulation was reduced (Sigman et al., 2010). On the other hand, Wunsch (2003) argued that reduced circulation during glacial periods is unlikely since increased wind-induced mixing may have favoured enhanced overturning.

Information regarding oceanic geochemistry and the temperature and/or the salinity of past water masses can be extracted from stable isotopes measured on benthic foraminifera tests that are contained in marine sediment cores. The distribution of the $\delta^{13}C$ of ΣCO_2 in the modern ocean is tightly linked to the oxygen and nutrient content, which are shaped by large-scale oceanic water mass movements (Kroopnick, 1985). Since the $\delta^{13}C$ of benthic foraminifera reflects the $\delta^{13}C$ of the Dissolved Inorganic Carbon (DIC) in seawater, past changes in the seawater oxygen and/or nutrient content can be reconstructed using the $\delta^{13}C$ obtained from benthic foraminifera tests in deep-sea sediments (Duplessy et al., 1984). On the other hand, the $\delta^{18}O$ of seawater ($\delta^{18}O_{sw}$) is related to salinity (Delaygue et al., 2000), and past changes in $\delta^{18}O_{sw}$ can be monitored using benthic foraminifera $\delta^{18}O$ (Zahn et al., 1991; Lynch-Stieglitz et al., 1999). However, the temperature fractionation that modulates the difference

* Corresponding author. Institute of Earth Sciences, Geology Department, Kiel University, Ludewig-Meyn-Str. 10 D-24118 Kiel, Germany.
E-mail address: gl@gpi.uni-kiel.de (G. Leduc).

0012-821X/$ – see front matter © 2010 Elsevier B.V. All rights reserved.
doi:10.1016/j.epsl.2010.08.002

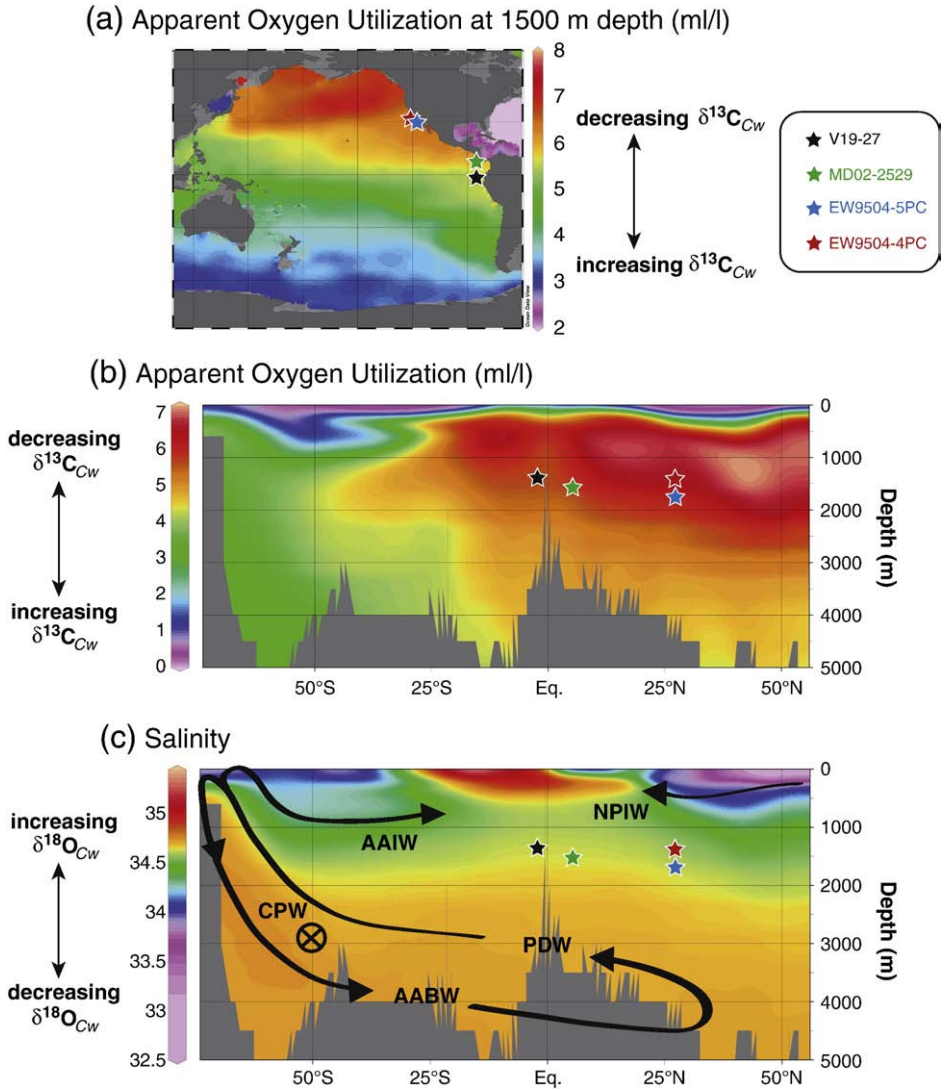

Fig. 1. (a) Map of Apparent Oxygen Utilization (AOU) distribution in the Pacific Ocean at 1500 m water depth. (b and c) Latitudinal transects of Eastern Pacific AOU and salinity, respectively. Coloured stars indicate the location of the sediment cores discussed in the text. The main pathways for Pacific water mass are indicated in the salinity transect. The main water mass are also indicated — NPIW indicates North Pacific Intermediate Water, AAIW indicates Antarctic Intermediate Water, AABW indicates Antarctic Bottom Water, PDW indicates Pacific Deep Water, and CPW indicates Circumpolar Water. Oceanic $\delta^{13}C$ and $\delta^{18}O$ are, respectively, related to AOU (Kroopnick, 1985) and salinity (Craig and Gordon, 1965). The AOU calculations and the salinity data are from Conkright and Boyer (2002). The figure was generated using the Ocean Data View software (http://odv.awi.de).

between the $\delta^{18}O_{sw}$ and the $\delta^{18}O$ of foraminifer tests, makes foraminifera $\delta^{18}O$ values a mixed signal for both temperature and $\delta^{18}O_{sw}$ (salinity).

The work described here makes a first attempt to jointly use benthic foraminifera $\delta^{13}C$ and $\delta^{18}O$ signatures in order to combine the information provided by each independently. We present a new high-resolution record of stable isotope measurements performed on epibenthic foraminifera that were obtained from a marine sediment core located in the Panama Basin (core MD02-2529, 08°12.33′N; 84°07.32′W; 1619 m water depth) that spans the past 150 kyr BP. The eastern equatorial Pacific (EEP) is situated at the confluence of northern suboxic and southern oxic waters at intermediate depths (Fig. 1). Therefore, studying past changes in water mass properties from this region will provide insights regarding how the North Pacific shadow zone has evolved in the past.

2. Modern-day Pacific Ocean circulation

In the modern North Pacific Ocean, relatively low sea surface salinities restrict North Pacific Intermediate Water (NPIW) formation to the upper 500 m of water depth (Warren, 1983; Talley, 1993; Reid, 1997; Emile-Geay et al., 2003, Fig. 1). Waters flowing below this depth have a remote southern component composed of a mixture of both NADW and waters originating from the Southern Ocean, at both intermediate (the Antarctic Intermediate Water, AAIW) and abyssal depths (the Antarctic Bottom Water, AABW) (Fig. 1, see also Reid, 1997). In the abyssal Pacific Ocean, the AABW density declines along its northward path as a result of heat diffusion from above and geothermal heating from below (Emile-Geay and Madec, 2009) and flows backwards as Pacific Deep Water (PDW) before upwelling at the Antarctic divergence (Fig. 1c). The circulation scheme leaves North Pacific waters situated between ~500 and ~2500 m depth within a shadow zone, where a sluggish ventilation leads to oxygen depletion in the entire North Pacific Ocean (Helly and Levin, 2004; Fiedler and Talley, 2006) (Fig. 1a).

Since intermediate waters do not ventilate the upper 1000 m (Fiedler and Talley, 2006), the EEP is almost anoxic below the main pycnocline. Also, high primary productivity induces intense deoxygenation rapidly below the euphotic layer, although ~90% of the organic matter derived from primary productivity is remineralized in the upper 200 m (Fiedler and Talley, 2006). Below 1000 m, anoxia is

not reached in the Panama Basin; however, suboxia still persists and results from a lack of ventilation at depth (Fiedler and Talley, 2006). The observed increase in Apparent Oxygen Utilization (AOU) from the southwestern to the northeastern Pacific, as depicted in Fig. 1a, provides a picture of water mass motion. Water enters in the Pacific Ocean from the south and confines the oldest Pacific waters to the northeastern Pacific (Fig. 1a) at these depths. The MD02-2529 coring site is located at the edge of northern oxygen-poor and southern oxygen-rich waters bathing the western American coastline, and is suitable for detecting the latitudinal extent of northeastern suboxic waters (Fig. 1b). A mapping of the radiocarbon circulation age for these water depths essentially provides the same picture (Matsumoto, 2007), which suggests that measuring benthic foraminifera $\delta^{13}C$ is appropriate for studying the scope of Pacific circulation and for tracking the latitudinal extent of the northeastern Pacific suboxic zone.

As compared to the above-described non-conservative tracers, there are no noticeable temperature and salinity latitudinal gradients in the eastern tropical Pacific at mid-depth (Fig. 1c). Tsuchiya and Talley (1996) showed a smooth density maximum for water depths at ~1500 m surrounding the equator that were linked to a broad salinity maximum at tropical latitudes (also see Fig. 1c). The salinity of northern and southern subtropical waters from the eastern Pacific at 1500 m was lower as compared to equatorial waters, while deeper waters were featureless (Fig. 1c). Since the oceanic density distribution determines large-scale water circulation, detecting past changes in basin-scale temperature and/or salinity gradients may provide important information regarding oceanic circulation rearrangements.

3. Pacific Ocean paleoceanography deduced from benthic $\delta^{13}C$ and $\delta^{18}O$

For the Last Glacial Maximum (LGM) time slice a deconvolution of temperature and salinity can be performed using an analysis of sedimentary pore water, for which salinity (chlorinity) together with benthic foraminifera stable isotopes and pore water $\delta^{18}O_{sw}$ measurements provide temperature and salinity estimations (Adkins et al., 2002). Such an analysis was performed on sediments collected from different oceanic basins and indicated that the deep ocean was uniformly cold, but that sharp salinity gradients existed between remote oceanic regions (Adkins et al., 2002). Mapping efforts attempting to characterize water mass geometry have revealed sharp gradients in water mass properties and nutrient concentrations at ~2000 m depth (Duplessy et al., 1988; Herguera et al., 1992; Keigwin, 1998; Matsumoto et al., 2002; Herguera et al., 2010). Duplessy et al. (1988), using a depth transect of benthic foraminifera $\delta^{13}C$, originally proposed that Glacial North Pacific Intermediate Water (GNPIW) formation occurred and occupied the 700 to 2600 m water depth range during the LGM. Other records from the northwestern Pacific suggest that GNPIW was characterized by lowered salinities (Keigwin, 1998). The coupling of benthic foraminifera $\delta^{13}C$ and Cd/Ca data, that accounts for the air–sea gas exchange imprint on the $\delta^{13}C$ of the surface ocean (Lynch-Stieglitz and Fairbanks, 1994), showed a North Pacific sourced water mass circulating at ~3000 m depth (i.e. significantly deeper than previously suggested by benthic foraminifera $\delta^{13}C$ alone). Recent evidence suggests that deep-water formation in the northern North Pacific occurred during the last deglaciation (Okazaki et al., 2010). Other North Pacific records have reported $\delta^{13}C$ increases for the last deglaciation that are comparable to the continental biomass contribution for mean oceanic $\delta^{13}C$ (Shackleton, 1977), arguing against drastic changes in deep Pacific circulation modes at glacial–interglacial timescales (Keigwin, 1987). The examples described illustrate a conundrum regarding the existence of GNPIW formation during the LGM.

On longer timescales, the alternation of laminated and bioturbated sediments in the Northeastern Pacific at ~500 m depth indicates abrupt changes in oxygenation synchronous with Greenland temperatures (Kennett and Ingram, 1995; Behl and Kennett, 1996; Ortiz et al., 2004; van Geen et al., 2003; Blanchet et al., 2007). Although productivity changes can explain these changes in oxygenation, both $\delta^{13}C$ data (Mix et al., 1999; Hendy and Kennett, 2003; Pahnke and Zahn, 2005) and model simulations (Mikolajewicz et al., 1997; Saenko et al., 2004) suggest that the Pacific Ocean circulation at intermediate depths may have been influenced by millennial-scale changes during the last glacial period.

The past behaviour of the North Pacific at mid-depth, hereafter referred to as the 1000 to 2000 m water depth range, remains elusive. Herguera et al. (2010) reported a deep redistribution of nutrients in the eastern Pacific during the LGM, pointing to a nutrient-rich water mass originating from northern high latitudes and circulating southward at mid-depth (Herguera et al., 2010). Over this time period, the northern Pacific shadow zone was likely ventilated by waters from a southern origin (Herguera et al., 2010). During the deglaciation, rapid changes in water mass advection, with a notable antiphase synchronicity between water masses at 800 and 1600 m depth (van Geen et al., 1996), were recorded simultaneously with rapid climate changes in the north Atlantic. On longer timescales, Stott et al. (2000a) found evidence of long-term changes in ventilation from a series of cores collected in silled basins along the California borderland, and observed a long-term increase in ventilation from late marine isotope stage (MIS) 4 to the LGM, while $\delta^{13}C$ values recorded during MIS5 and early MIS4 were comparatively higher.

At deeper sites (~3000 m), Northeastern and Southeastern Pacific ventilation changes were similarly influenced by rapid climate changes that occurred during the last glacial period (Lund and Mix, 1998; Ninnemann and Charles, 2002) in antiphase with North Atlantic $\delta^{13}C$ records (see e.g. Vidal et al., 1997). Whether increases in North Pacific deep-water ventilation originated from "above" or "below" still remains elusive (see discussion in Lund and Mix, 1998). However, they are likely linked to millennial-scale changes in the strength of ocean stratification occurring at mid-depth (Charles et al., 2010).

4. Methods

We measured stable carbon and oxygen isotopes on the benthic foraminifer species *Cibicidoides wuellerstorfi*, and on the planktonic foraminifera species *Globigerinoides ruber* and *Neogloboquadrina dutertrei* in the >250 μm size fraction in MD02-2529 core. Samples containing one to four benthic foraminifera and two to six planktonic foraminifera were treated with H_3PO_4 at 70 °C. The resulting CO_2 was analysed using a Finnigan Delta Advantage mass spectrometer at CEREGE. We performed ~20 replicates on a total of ~400 measurements for benthic foraminifera, especially at key depths where rapid isotopic shifts were recorded (see Supplementary materials). Replicates indicated that the rapid isotopic shifts we describe below are robust. Stable isotopic ratios are reported in ‰ relative to V-PDB. The analytical precision, based on repeated analyses of a NBS-19 limestone standard, was ±0.05‰ for $\delta^{18}O$ and ±0.03‰ for $\delta^{13}C$ (±1σ).

The total carbon and the organic carbon sedimentary content were measured with a CNS elemental analyser, FISONS 1500. The standard used for C_{org} was an Acetanilide powder (C_8H_9NO, containing 71.09% carbon). The analytical precision was better than ±5%. Carbonate removal was accomplished by successive additions of HCl at 0.1 M. Each value of organic carbon shown represents the mean of two measurements. The Calcium Carbonate sedimentary content (% $CaCO_3$) was estimated using the following equation:

$$\%CaCO_3 = \left(\%C_{tot} - \%C_{org}\right)^{*}8.33$$

Total C_{37} alkenones were extracted using the procedure fully described in Sonzogni et al. (1997) and Pailler and Bard (2002). C_{37}

alkenone concentrations are used as a proxy for coccolithophorid productivity. All of the measurements were performed at CEREGE.

The age model for core MD02-2529 was based on calibrated radiocarbon ages for the last 40 kyr BP, and on the benthic foraminifera stratigraphy for the rest of the sequence (Leduc et al., 2007). For conversion of the ^{14}C ages into calendar ages, we used the MARINE04 calibration curve to 26 kyr BP (Hughen et al., 2004), and the equation published in Bard et al. (2004), computed with respect to GISP2 chronology (Stuiver and Grootes, 2000), for older ages. We tuned the broad $\delta^{18}O$ minima of our benthic records to the Antarctic warm events recorded in the $\delta^{18}O$ of Byrd ice core (Blunier and Brook, 2001) for the MIS3 and to a benthic oxygen isotope stack for the 60–150 kyr BP time period (Lisiecki and Raymo, 2005). Overall, sedimentation rates of ~10 cm kyr^{-1} remained constant throughout the last glacial period. The temporal resolution was ~300 years for the 0–65 kyr BP time interval, and ~1000 years for the 65–150 kyr BP time interval.

5. Results

5.1. Patterns and significance of the C. wuellerstorfi isotopic signatures

With epibenthic foraminifera considered as oxic taxa (see e.g. Jorissen, 1999), the presence of *C. wuellerstorfi* throughout the sedimentary sequence indicates that bottom water oxygen concentrations never reached dysoxic values over the time interval studied (Fig. 2). The $\delta^{18}O$ of *C. wuellerstorfi* ($\delta^{18}O_{Cw}$) for the last 10 kyr BP was ~2.6 ± 0.1‰ (Fig. 2). Between 10 and 20 kyr BP, the last glacial termination was marked by a $\delta^{18}O_{Cw}$ increase of ~2‰ (Fig. 2). MIS2

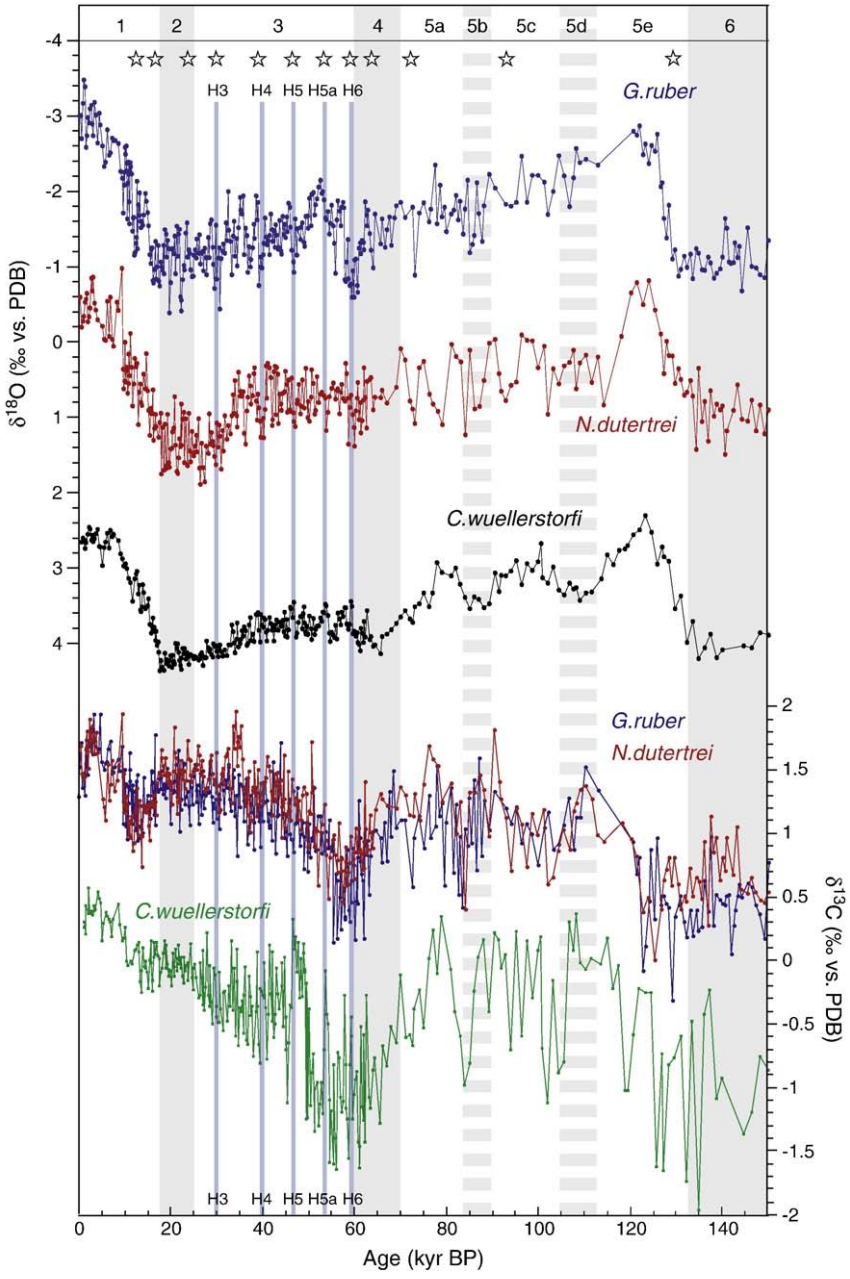

Fig. 2. Stable isotopes measured for the last 150 kyr BP on planktonic foraminifera (*G. ruber* and *N. dutertrei* $\delta^{13}C$ in blue and red, respectively) and benthic foraminifera (*C. wuellerstorfi* $\delta^{13}C$ in green, $\delta^{18}O$ in black) from core MD02-2529. Marine isotope stages are marked by gray bars and labelled at the top of panel. Heinrich events occurring during MIS3 are marked by blue bars. Periods of increases in planktonic $\delta^{18}O$, likely connected to North Atlantic cold periods, are marked by the black stars.

values of benthic $\delta^{18}O$ remained rather constant (Fig. 2). The 30–70 kyr BP time interval was marked by $\delta^{18}O_{Cw}$ variations of ~0.2 to 0.5‰ on the millennial timescale (Fig. 2). The 70–140 kyr BP time interval exhibited long-term variations generally observed in deep-sea oxygen isotopic sequences during MIS5 (Fig. 2). Several $\delta^{18}O_{Cw}$ minima were recorded during the last glacial period during times of *G. ruber* $\delta^{18}O$ maxima that corresponded to Heinrich events and/or to Greenland cold stadials (Fig. 2, see Leduc et al., 2007).

The $\delta^{13}C$ of *C. wuellerstorfi* ($\delta^{13}C_{Cw}$) for the last 25 kyr BP remained quite constant, with the notable exception of a step-like $\delta^{13}C_{Cw}$ decrease of ~0.3‰ that occurred at ~11 kyr BP (Fig. 2). The MIS3 $\delta^{13}C_{Cw}$ record was then marked by millennial-scale fluctuations that were amplified toward MIS4, attaining amplitudes of ~1‰ between 40 and 65 kyr BP (Fig. 2). On this rapid variability, a $\delta^{13}C$ decreasing trend of ~1‰ is superimposed, with a step-like decrease in mean $\delta^{13}C_{Cw}$ values recorded at ~50 kyr BP (Fig. 2). The lower $\delta^{13}C_{Cw}$ resolution record for MIS5 seems to be as variable as MIS3, with well-marked negative $\delta^{13}C$ anomalies centred at the MIS 5a/5b, 5c/5d, and 5e/6 boundaries (Fig. 2). $\delta^{13}C_{Cw}$ values recorded during the MIS6 glacial maximum were much lower than those recorded during MIS2.

In high biological productivity environments, $\delta^{13}C_{Cw}$ can be lowered by respiration (due to organic matter oxidation) within the sediment (Stott et al., 2000b) and/or at the water–sediment interface (Mackensen et al., 1993). We sought to determine if influences in productivity changes for $\delta^{13}C_{Cw}$ could explain some of the time windows when very low and variable $\delta^{13}C_{Cw}$ were recorded. For this determination, we compared the $\delta^{13}C_{Cw}$ to downcore measurements in the C_{org} content, the alkenone concentrations, and the $CaCO_3$ content (Fig. 3) measured on the same core.

Overall, MD02-2529 productivity proxies suggest that export productivity has increased during glacial stages and during shorter time intervals for MIS 3 and 4, but that they cannot explain either the long-term or the millennial-scale $\delta^{13}C_{Cw}$ shifts that have occurred during the past 140 kyr BP (Fig. 3). In particular, the high $\delta^{13}C_{Cw}$ that was recorded during MIS2, and the low $\delta^{13}C_{Cw}$ that was recorded during MIS4/early MIS3 were not satisfactorily correlated with any of the productivity proxies. Also, the highly variable $\delta^{13}C_{Cw}$ recorded during the MIS4/early MIS3 time interval did not seem to be linked to rapid changes in productivity (Fig. 3). Conversely, the most prominent changes in C_{org} bracketing MIS2 corresponded to very stable and high $\delta^{13}C_{Cw}$ (Fig. 3). The MD02-2529 core location lies below the most stratified upper waters of the world ocean. Studies that focused on pycnocline and nutricline variability spanning the last glacial period suggest that this stratification was efficient in the past (Leduc et al., 2007, 2009).

Through postdepositional carbonate overgrowth in the low $\delta^{13}C_{DIC}$ of pore waters, recrystallization can also alter $\delta^{13}C_{Cw}$ (McCorkle et al.,

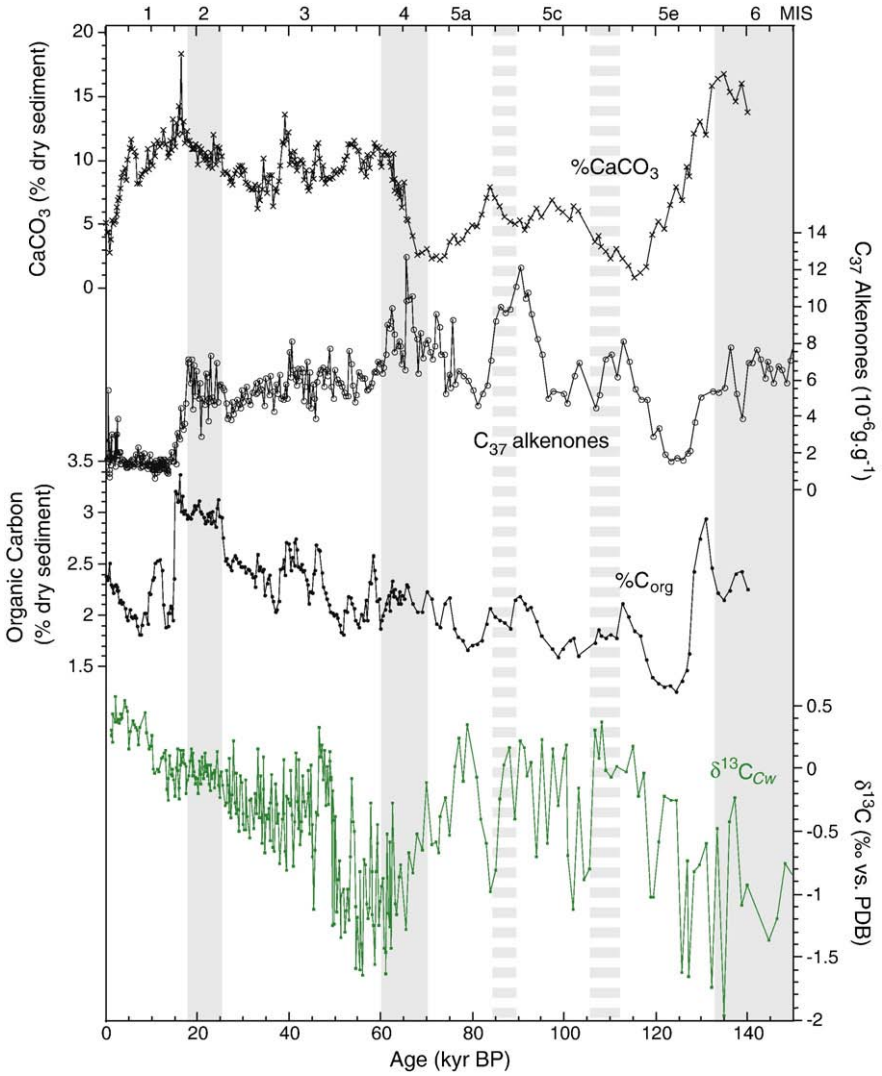

Fig. 3. Comparison between temporal variations of $\delta^{13}C_{Cw}$ (green curve, bottom panel) and paleoproductivity proxies in MD02-2529 (black curves, upper panels), with black dots, open circles, and crosses corresponding to the sedimentary organic carbon content, the sedimentary C_{37} alkenone concentrations, and the sedimentary $CaCO_3$ content, respectively. Marine isotope stages are labelled at the top of the figure.

1985; Torres et al., 2003). Since the structures of porous planktonic foraminiferal tests make them more prone to diagenetic recrystallization than benthic foraminifera (Pearson et al., 2001), we examined our planktonic $\delta^{13}C$ records. In MD02-2529, the downcore $\delta^{13}C$ changes recorded by *G. ruber* and *N. dutertrei* were much smoother than those of *C. wuellerstorfi* (Fig. 2), and on the same order as for other marine sediment cores located further south (Spero et al., 2003; Pena et al., 2008). Therefore, the planktonic foraminifera $\delta^{13}C$ signatures are likely linked to the eastward advection of subsurface waters coming from the subtropics (Gu and Philander, 1997). Long-term trends observed for both benthic and planktonic $\delta^{13}C$ records can be linked to changes in the global oceanic $\delta^{13}C$ of the ΣCO_2 pool, which are triggered by changes in the terrestrial biosphere (Shackleton, 1977). However, neither the long-term nor the millennial-scale MD02-2529 $\delta^{13}C_{Cw}$ that attained 1‰ could be imputed to authigenic recrystallization and/or to changes in the land biosphere. Therefore, we conclude that the MD02-2529 $\delta^{13}C_{Cw}$ signature and upper oceanic productivity and stratification records were decoupled, and use MD02-2529 $\delta^{13}C_{Cw}$ as a proxy for ambient seawater $\delta^{13}C_{DIC}$.

5.2. On the relationship between $\delta^{13}C_{Cw}$ and $\delta^{18}O_{Cw}$

A striking feature from MD02-2529 benthic foraminifera stable isotopic records was the amplitude and the sharpness of the variability in $\delta^{13}C_{Cw}$, and to a lesser extent, in $\delta^{18}O_{Cw}$ during the last glacial period. To clarify the nature of these variabilities we investigated whether $\delta^{13}C_{Cw}$ and $\delta^{18}O_{Cw}$ anomalies were interrelated. Millennial-scale $\delta^{13}C_{Cw}$ and $\delta^{18}O_{Cw}$ changes were extracted by subtracting the five-point running average from the raw isotopic datasets in order to capture rapid changes in $\delta^{13}C_{Cw}$ and $\delta^{18}O_{Cw}$ (Fig. 4a). In Fig. 4c, these $\delta^{13}C_{Cw}$ and $\delta^{18}O_{Cw}$ anomalies are reported for the 25–65 kyr BP time interval. Both the $\delta^{13}C_{Cw}$ and $\delta^{18}O_{Cw}$ excursions were broadly negatively correlated over this time interval with a $\Delta\delta^{13}C/\Delta\delta^{18}O$ slope of ~−3, and with a level of significance higher than 99.5% for that time interval (Fig. 4c, d). Replicates performed on benthic foraminifera during this time interval confirm the negative relationship shown in Fig. 4c and d (see Supplementary materials). The $\Delta\delta^{13}C/\Delta\delta^{18}O$ feature has several important implications regarding the reliability of the isotopic records, and the hydrological mechanisms responsible for the origin of the $\delta^{13}C/\delta^{18}O$ relationship.

First, both the $\delta^{13}C_{Cw}$ and the $\delta^{18}O_{Cw}$ could be influenced by dissolution (Wu and Berger, 1989), by carbonate ion concentrations (Spero et al., 1997), and by vital effects (Adkins et al., 2003). For these cases, the $\delta^{13}C_{Cw}$ and the $\delta^{18}O_{Cw}$ are expected to covary positively. A negative relationship between millennial-scale $\delta^{13}C_{Cw}$ and $\delta^{18}O_{Cw}$ excursions (Fig. 4c) indicates that other processes linked to hydrological changes at the core location drove these isotopic excursions on the millennial timescale. Second, if the expansion and contraction of high-nutrient water masses such as those in the present-day OMZ were driven by changes in organic matter remineralization alone, then both $\delta^{13}C_{Cw}$ and $\delta^{18}O_{Cw}$ would be expected to evolve independently, with $\delta^{18}O_{Cw}$ being uninfluenced by this phenomenon. Instead, both of these records are strikingly linked (Fig. 4b, c) suggesting that temperature and/or $\delta^{18}O_{sw}$ changed synchronously with the $\delta^{13}C_{DIC}$ of ambient seawater in relation to water masses of various temperatures and salinities.

In Fig. 4b we determined whether or not the broad negative relationship between $\delta^{18}O_{Cw}$ and $\delta^{13}C_{Cw}$ was a robust feature for the entire record. We computed temporal variations of the Pearson linear correlation coefficient (r^2) for anomalies, extracted from Fig. 4a, for the last 150 kyr BP (Fig. 4b). We used five pairs of $\delta^{18}O_{Cw}$ and $\delta^{13}C_{Cw}$ anomalies in order to calculate the r^2 that was symmetrically distributed surrounding each r^2 value (Fig. 4b). Fig. 4b provides a picture of the past changes in the coupling between both the $\delta^{18}O_{Cw}$ and $\delta^{13}C_{Cw}$ anomalies on millennial timescales.

If the r^2 values were randomly scattered around zero, there would be no noticeable relationship between both rapid $\delta^{18}O_{Cw}$ and $\delta^{13}C_{Cw}$ shifts. From Fig. 4b it appears that during most of the last glacial–interglacial cycle, the correlation between $\delta^{18}O_{Cw}$ and $\delta^{13}C_{Cw}$ anomalies was negative. It indicates that waters bathing the MD02-2529 coring site alternately shifted from a nutrient-rich water mass (with a low $\delta^{13}C_{DIC}$) of lower temperature and/or higher salinity (as recorded by higher $\delta^{18}O_{Cw}$) compared to another nutrient-poor water mass characterized by relatively high $\delta^{13}C_{Cw}$ anomalies. The trend is particularly apparent for MIS 6, 5e, 5c, 4, and for the 25–45 kyr BP time intervals when r^2 values fall above the 95% confidence level.

6. Discussion

6.1. The origin and extent of glacial EEP water masses at mid-depth

One valid explanation for long-term and rapid variations in $\delta^{13}C_{Cw}$ recorded during the last glacial period in core MD02-2529 potentially lies in long-term and rapid movements of a sharp water mass front located in the vicinity of the coring site at approximately 1600 m water depth. To test this hypothesis we first compared epibenthic foraminiferal $\delta^{13}C$ records available from the north and the south of the MD02-2529 core location in the 1400 to 1800 m water depth range (Fig. 1).

The sediment core situated at the equator (core V19-27, 1373 m depth, Fig. 1) is marked by very stable and high $\delta^{13}C_{Cw}$ values spanning the last 150 kyr BP as compared to MD02-2529 $\delta^{13}C_{Cw}$ values (Mix et al., 1991) (Fig. 5). Two cores collected in California silled basins (cores EW9504-04PC, sill at 1400 m depth; and EW9504-05PC, sill at 1815 m depth, Fig. 1) exhibit $\delta^{13}C$ values lower by ~1‰ than for the $\delta^{13}C_{Cw}$ recorded in V19-27 for the last 150 kyr BP (Stott et al., 2000a, Fig. 5). The latitudinal offset indicates that the contrast observed nowadays in nutrient concentrations has persisted in the eastern Pacific at mid-depths over the last glacial–interglacial cycle. A sharp $\delta^{13}C_{DIC}$ gradient separating these water masses may have existed along the northwestern Mexican Margin, and was likely confined somewhere between 30°N and the equator.

The Panama Basin is located between these two latitudes, making the MD02-2529 coring site potentially sensitive to the latitudinal extent of these northern and southern end-members. V19-27 and MD02-2529 were apparently bathed by the same southern origin water masses over the last 25 kyr BP (Fig. 5), as suggested by a common $\delta^{13}C_{Cw}$ evolution during this time period, which indicates that the latitudinal gradient in AOU observed nowadays at mid-depth (Fig. 1) remained mostly north of the MD02-2529 core location during MIS2 as well (see also Herguera et al., 2010). Older periods were marked by rapid and high-amplitude $\delta^{13}C_{Cw}$ shifts in MD02-2529 between $\delta^{13}C$ values for northern and southern end-members, which are interpreted as reflective of displacements in the water mass front separating both the northern and southern water masses (Fig. 5). The 50–70 kyr BP and some time intervals spanning MIS5 and 6, when MD02-2529 $\delta^{13}C_{Cw}$ values dropped to −1‰, suggest that the Panama Basin was under the influence of northern nutrient-rich waters at mid-depth. In particular, California silled basin cores share low $\delta^{13}C$ signatures with MD02-2529 as recorded over the MIS4–early MIS3 time interval when MD02-2529 was mostly influenced by the northern end-member water mass, while V19-27 $\delta^{13}C_{Cw}$ values remained stable (Fig. 5). The long-term $\delta^{13}C$ increasing trend recorded in MIS4 and in early MIS3 in the northeastern Pacific by the EW9504 cores has been explained by an increase in ventilation at mid-depth (Stott et al., 2000a). In the MD02-2529 core this trend is somewhat amplified since an increase in the frequency of southern water mass incursions within the Panama Basin is superimposed on the long-term $\delta^{13}C_{Cw}$ trend recorded in EW9504 cores (Fig. 5). The $\delta^{13}C$ anomaly found in both EW9504 and MD02-2529 cores, but not in V19-27, suggests that a shift in the $\delta^{13}C$ pool of northern end-member

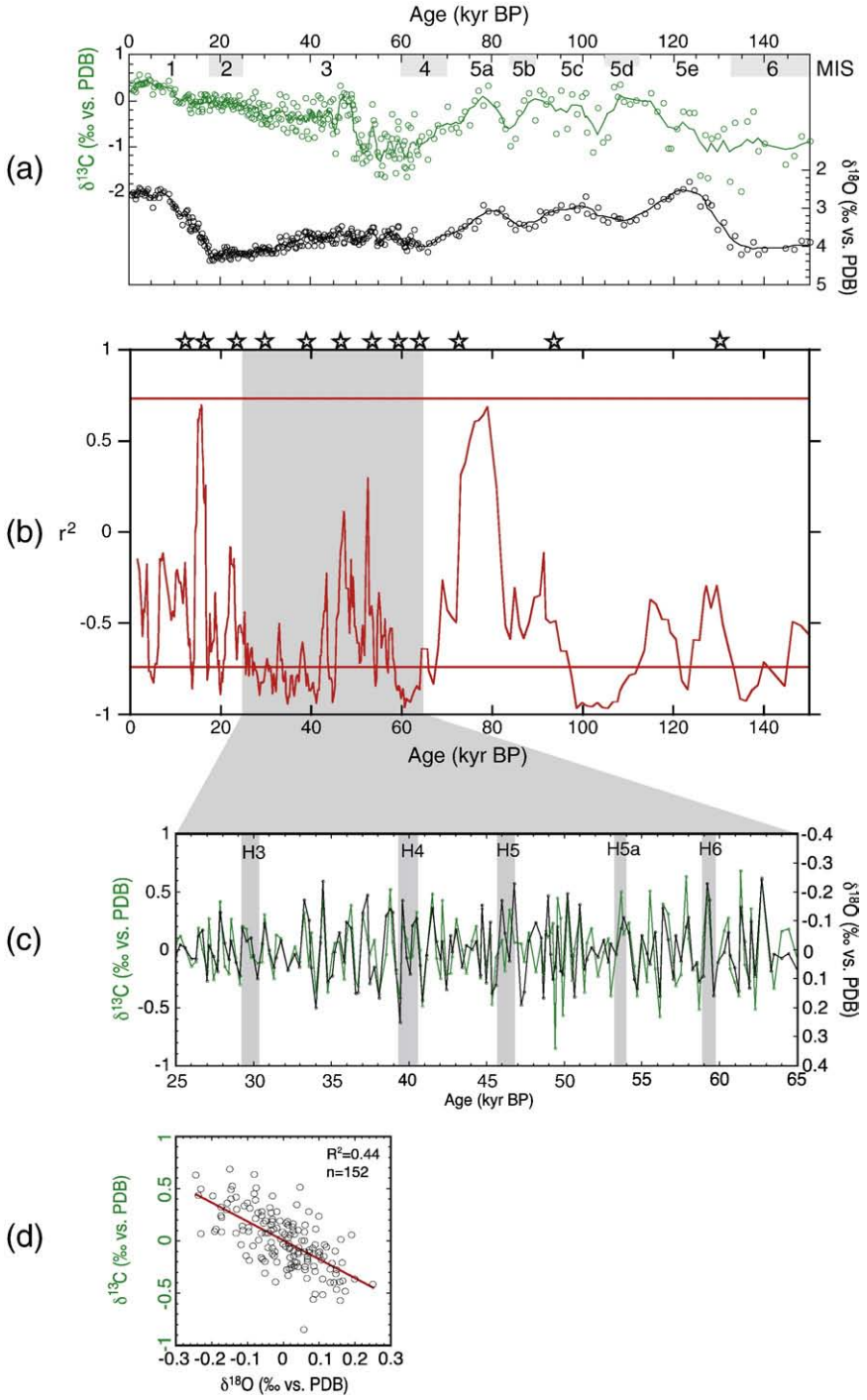

Fig. 4. The extraction and statistical significance of the $\delta^{13}C_{Cw}$ and $\delta^{18}O_{Cw}$ centennial anomalies in MD02-2529. (a) $\delta^{13}C_{Cw}$ (green open circles) and $\delta^{18}O_{Cw}$ (black open circles), as well as the five-point running average calculated for each dataset (green and black curves). The anomalies were calculated by subtracting the five-point running average from the raw data. Marine isotope stages are labelled at the top of the panel. (b) Temporal variations of the correlation coefficient (r^2) calculated using five pairs of $\delta^{13}C_{Cw}$ and $\delta^{18}O_{Cw}$ anomalies. According to the temporal resolution determined during MIS3, the r^2 determined during this time interval provided a correlation coefficient over temporal windows of ~1250 years, centred on each r^2 value. The horizontal red lines provide r^2 threshold values for which the correlation was significant at a 95% confidence level. Periods of increases in planktonic $\delta^{18}O$ likely connected to North Atlantic cold periods are marked by black stars, as seen in Fig. 2. (c) Temporal variations of $\delta^{13}C$ (green) and $\delta^{18}O$ (black) anomalies for the 25–65 kyr BP time interval. (d) Relationship between $\delta^{13}C$ and $\delta^{18}O$ anomalies shown in panel c. Note that the r^2 calculation for $\delta^{13}C$ and $\delta^{18}O$ anomalies shown in panel d (with 150 degrees of freedom) is significant at a confidence level higher than 99.5%. Vertical lines shown in c localize the Heinrich events as depicted in Fig. 2.

waters impacted the northeastern Pacific over MIS4 and 3, but apparently did not reach the southern hemisphere (Fig. 5).

We also observed negative MD02-2529 $\delta^{13}C_{Cw}$ overshoots with respect to $\delta^{13}C_{DIC}$ values for the northern end-member during early MIS3 and MIS5. The offset can be explained by several processes such as the following: (1) the sampling strategy for MD02-2529 — which may have lead to a higher noise level since one to four specimens were analyzed in MD02-2529 vs. 10 to 20 specimens for California borderlands cores (Stott et al., 2000a); (2) some species-specific vital effects — due to the fact that another *Cibicides* species was used in California borderlands (*Cibicides mckannai*); and (3) a $\delta^{13}C_{DIC}$ lowering — due to organic matter remineralization in the water

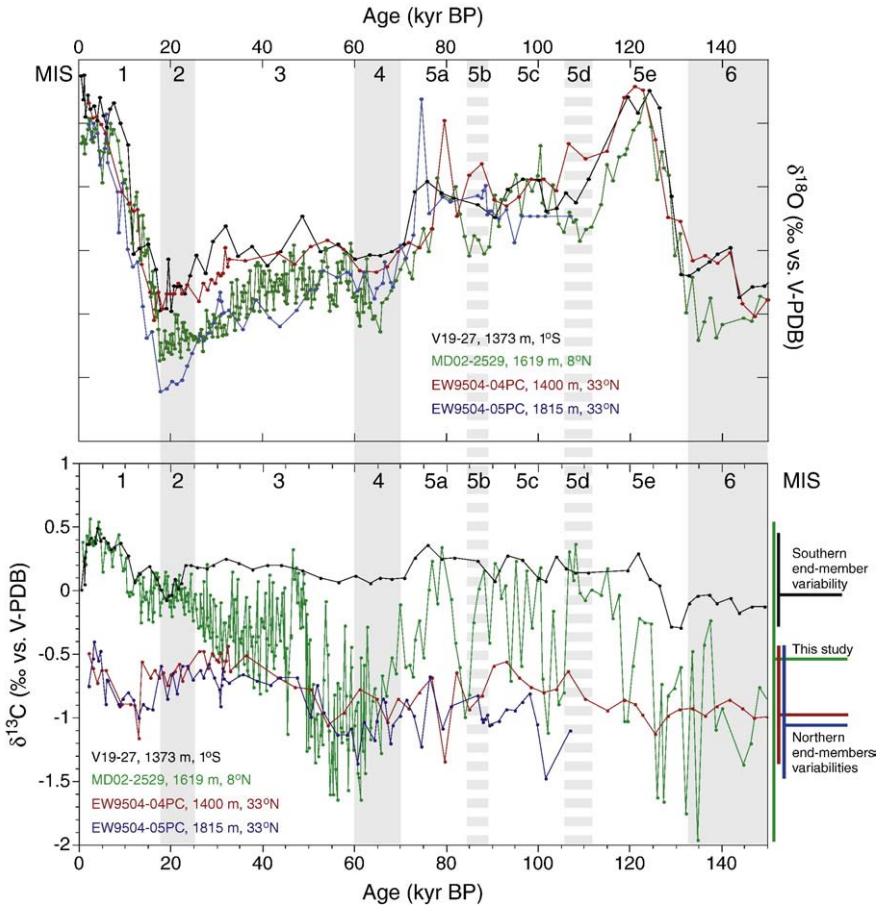

Fig. 5. Temporal variations for $\delta^{18}O$ (upper panel) and $\delta^{13}C$ (lower panel) measured on epibenthic species (namely *C. wuellerstorfi* for cores MD02-2529 (this study) and V19-27 (Mix et al., 1991) and *Cibicides mckannai* for cores EW9504-04PC and EW9504-05PC (Stott et al., 2000a)) in the mid-depth Eastern Pacific at different latitudes. The $\delta^{13}C$ measured on *C. mckannai* was corrected by −0.3‰ in order to account for the positive offset between the $\delta^{13}C$ of *C. mckannai* and the $\delta^{13}C_{DIC}$ (Stott et al., 2000a) while the $\delta^{13}C_{Cw}$ is likely to properly reflect $\delta^{13}C_{DIC}$ (Duplessy et al., 1984). The marine isotope stages are labelled at the top of the figure.

column that could have occurred along the water mass path between the California borderlands and the Panama Basin.

From the original publication of Stott et al. (2000a), six cores in total are documenting the 1000 to 2000 m water depth range from California silled basins spanning the last glacial period. When all of these cores are considered, low $\delta^{13}C$ values during MIS4 followed by an increasing $\delta^{13}C$ trend documented for MIS3 were clearly apparent within the 1200 to 2000 m water depth range (Fig. 6). On the other hand, two shallower cores from the 1000 to 1200 m depth range were marked by only subtle $\delta^{13}C$ changes during these time intervals (Fig. 6). The observation suggests that the MD02-2529 negative $\delta^{13}C$ excursion that occurred between 70 and 50 kyr BP could be related to some oceanographic features identified upstream on the California Margin. Likely is that the changes observed in $\delta^{13}C_{DIC}$ for the northern end-member water mass mark a firm upper limit at ~1200 m as revealed by the depth transect from the California Margin (Fig. 6). The water mass boundary lying at ~1200 m water depth may also explain the divergent $\delta^{13}C$ trends spanning the last 15 kyr BP along the California margin (Fig. 6). Within the 1200 to 2000 m depth range, the $\delta^{13}C$ signal from California Margin cores dropped to values much lower than the $\delta^{13}C$ values recorded in MD02-2529 during the last deglaciation time interval. This feature confirms that the hydrological boundary separating the northern and southern water mass was located north of the MD02-2529 core location, as indicated by identical MD02-2529 and V19-27 $\delta^{13}C_{Cw}$ evolutions spanning the last 25 kyr BP (Fig. 5).

Decreases in $\delta^{13}C_{Cw}$, recorded at the MD02-2529 site prior to 25 kyr BP, can be explained by a southward spreading of the northern water mass end-member that was located further north from 25 kyr BP onwards. Such a southward nutrient-rich water mass extent could be interpreted as either a reinvigoration of north Pacific water circulation at depth during the last glacial period, or as the reduced extent of the southern, nutrient-poor end-member, likely resulting in less water advection from the south during these time periods.

At present, no clear evidence for sustained GNPIW formation spanning the last glacial period is available. However, regional climate characteristics and sedimentary processes from the Okhotsk Sea (Gorbarenko et al., 2010), the Bering Sea (VanLaningham et al., 2009; Horikawa et al., 2010), and the Gulf of Alaska (Zahn et al., 1991) remain potential sites where GNPIW formation could have occurred. Ideally, benthic foraminiferal isotopic evidence for deep-water formation in the northern North Pacific at high latitudes is required in order to confirm the existence of the GNPIW responsible for the $\delta^{13}C$ anomaly recorded at mid and low latitudes along the western American Margin. Counter-intuitively, our data suggest that an increase in GNPIW formation would not necessarily lead to relatively high $\delta^{13}C$ signatures if GNPIW formation had spread as far as tropical latitudes by ~1500 m water depth.

6.2. Northern vs. Southern hydrological contrasts during the last glacial period

The negative correlation between $\delta^{18}O_{Cw}$ and $\delta^{13}C_{Cw}$ anomalies implies that the northern nutrient-rich (low $\delta^{13}C$) water mass end-member was either colder, or of higher $\delta^{18}O_{sw}$ (salinity) for time

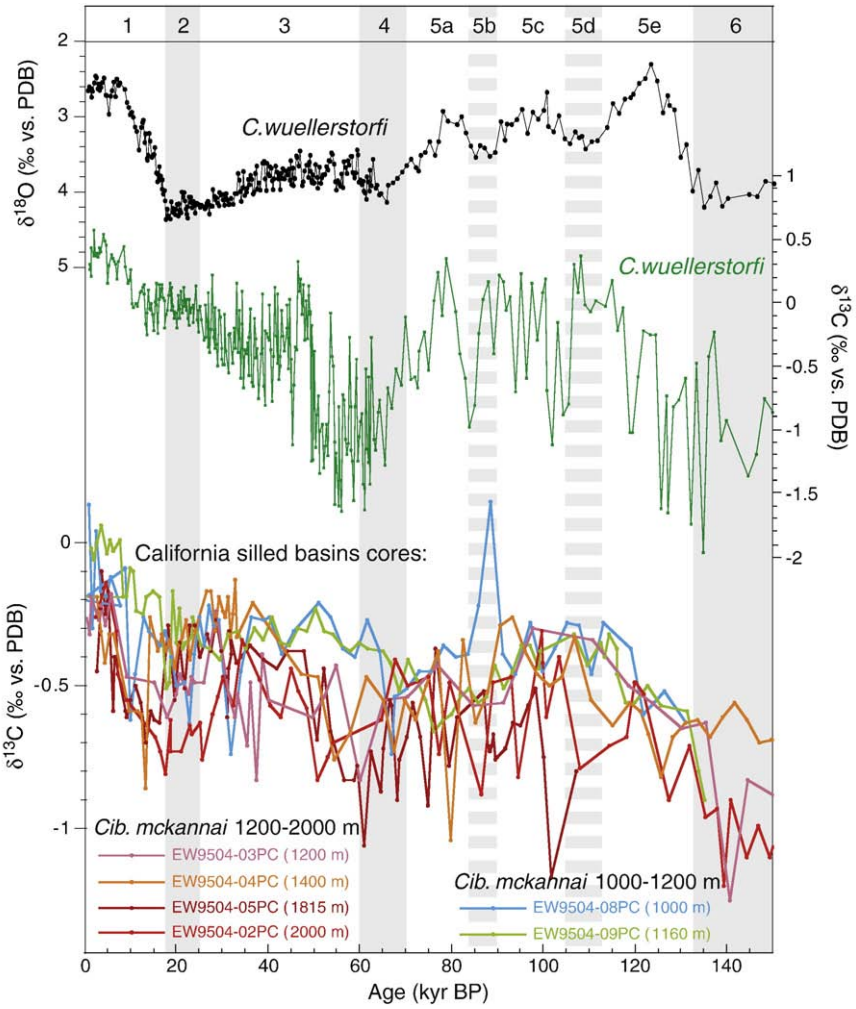

Fig. 6. Upper panels: temporal variations of $\delta^{18}O$ (black line) and $\delta^{13}C$ (green line) measured in core MD02-2529. Lower panels: epibenthic $\delta^{13}C$ measurements performed on *C. mckannai* in cores from Southern California silled basins (Stott et al., 2000a). Note the divergent $\delta^{13}C$ trends observed in the cores in the 1000 to 1200 m water depth range as compared to those from the 1200 to 2000 m range recorded for the last 15 kyr BP, as well as for the 70–50 kyr BP time interval.

periods when negative r^2 are recorded, and vice-versa for the water mass with a southern origin (Fig. 4b). Not surprisingly, the negative correlation was found to be strongest when MD02-2529 $\delta^{13}C_{Cw}$ values were highly variable and/or when they were in between both of the water masses end-members (as, for example, between 25 and 45 kyr BP and surrounding 100 kyr BP (Figs. 4b, and 5)). In other words, the alternative influence of the two end-members at the MD02-2529 coring site potentially generates anomalies with significant high/low r^2 values, while any correlation is observed when one water mass predominates, as, for example, over the last 25 kyr BP (Fig. 4b).

When the MD02-2529 record is compared to the benthic foraminiferal $\delta^{18}O$ of the northern and southern end-members, it appears that vertical density gradients best explain the benthic $\delta^{18}O$ differences among cores during the last glacial period, as presented in Fig. 5. Although multi-millennial MD02-2529 $\delta^{18}O_{Cw}$ changes can be partly linked to variations in ice volume (Siddall et al., 2008), centennial to millennial-scale $\delta^{13}C_{Cw}$ anomalies prior to 25 kyr BP are still clearly associated with local changes in temperature and seawater $\delta^{18}O$ (Fig. 4). We argue that oxygen and carbon isotopic covariations at the millennial timescale are a robust indication for the influence of two contrasted water masses in terms of $\delta^{13}C_{DIC}$ and $\delta^{18}O_{sw}$ and/or temperature at the core location.

The two water mass end-members existing during MIS3 left oxygen isotope fingerprints with different signatures of up to 0.5‰ in $\delta^{18}O_{Cw}$. Supposing a constant $\delta^{18}O_{sw}$/salinity relationship, the $\delta^{18}O_{Cw}$ shifts translate to temperature or salinity contrasts in the glacial eastern Pacific at mid-depth of up to ~2.5 °C or ~1.5 practical salinity units, respectively. Waters with a northern origin were likely colder and/or saltier, and arguably denser (Lynch-Stieglitz et al., 1999). Pore water measurements indicate that the density fields were characterized by heterogeneous salinities rather than by temperature gradients during the LGM (Adkins et al., 2002). We are fully aware of the complications linked to the fact that deep-water formation through sea-ice formation and brine rejection may have strongly influenced the $\delta^{18}O_{sw}$/salinity relationship (see e.g. McCave et al., 2008; Ganopolski and Roche, 2009), as well as that some temperature influences cannot be ruled out. However, we support the interpretation of sub-millennial $\delta^{18}O_{Cw}$ variations in terms of regional changes in $\delta^{18}O_{sw}$ and relate it to a salinity gradient that existed in the eastern Pacific at mid-depths during the last glacial period.

In an attempt to reconstruct northwestern Pacific LGM hydrology from a core depth transect, Keigwin (1998) argued that low-salinity waters were formed in the Okhotsk Sea and spread at mid-depth, as formerly referred to by Duplessy et al. (1988) for GNPIW. The MD02-2529 results provide, for the first time, an opportunity to distinguish the sign of the salinity gradients that existed between distant Glacial Pacific water masses at mid-depth in the eastern Pacific. The negative correlation between $\delta^{18}O_{Cw}$ and $\delta^{13}C_{Cw}$ reported in MD02-2529 suggests that waters of southern origin advecting toward the

MD02-2529 coring site were fresher than waters of northern origin during the last glacial period.

6.3. Timing of changes in water mass circulation and properties spanning the last 150 kyr BP

The long-term evolution of the origin of waters spreading in the Panama Basin is clearly decoupled from changes in ice volume (e.g. the last 25 kyr BP indicates a southern origin throughout the Holocene and MIS2 time periods (Fig. 5)). However, during MIS3 we did find some evidences for positive $\delta^{13}C_{Cw}$ excursions during Heinrich events (Fig. 2) that were also previously identified in the benthic $\delta^{18}O$ records and that were used to tune those records to the Byrd ice core in order to construct the age model (Leduc et al., 2007).

Millennial-scale climate events such as those characterizing the last glacial–interglacial cycle are linked to rapid changes in both nutrient and temperature gradients between intermediate and deep Southern Ocean water masses (Charles et al., 2010). Heinrich events, for example, are marked by reduced nutrient content and warmer temperatures in the Southern Ocean at intermediate depths as compared to warm interstadials. Although the mechanism described by Charles et al. (2010) may have acted to enhance the millennial-scale MD02-2529 $\delta^{13}C_{Cw}$ and $\delta^{18}O_{Cw}$ anomalies, it clearly cannot explain the magnitudes observed in MD02-2529 isotopic shifts. Additionally, a deeper core from EEP (core RC13-110, Mix et al., 1991) did not exhibit $\delta^{13}C_{Cw}$ values low enough to invoke changes in vertical nutrient gradients as described in Charles et al. (2010) that would help to explain the MD02-2529 $\delta^{13}C_{Cw}$ record. Smooth latitudinal changes of a sharp water mass front are more likely responsible for the millennial-scale shifts observed in MD02-2529 benthic isotope records.

Positive MD02-2529 $\delta^{13}C_{Cw}$ anomalies likely reflect the northward spreading of AAIW during Heinrich events, as previously reported (Schulte et al., 1999; Pahnke and Zahn, 2005; Pichevin et al., 2007; Jung et al., 2009). Although very few benthic foraminifera records from the Eastern Pacific have sufficient time resolution to document millennial-scale changes in oceanic circulation, they all suggest that during Heinrich events the intermediate to deep Pacific circulation was enhanced (see Lund and Mix, 1998 for the deep Northeastern Pacific; Ninnemann and Charles, 2002 for the deep Southeastern Pacific; Hendy and Kennett, 2003 and Blanchet et al., 2009 for Santa Barbara Basin).

In MD02-2529, millennial-scale *G. ruber* $\delta^{18}O$ increases are likely related to periods when surface waters from the North Atlantic were influenced by freshwater fluxes, such as, for example, during Heinrich events for MIS3. During most of these time intervals, the sign of covariation for isotopic anomalies seems to have been reversed (Fig. 4b, c). Some r^2 excursions suggest that $\delta^{18}O_{Cw}$ and $\delta^{13}C_{Cw}$ correlations could have been positive during terminations, during the MIS5a glacial inception, as well as over short time periods coincident with some Heinrich events during MIS3 (Fig. 4b, also see the Supplementary materials for r^2 calculated over different numbers of $\delta^{13}C_{Cw}$ and $\delta^{18}O_{Cw}$ pairs). From the replicates that we measured within the 25–65 kyr BP time interval, only four replicates were found to exhibit higher $\delta^{13}C_{Cw}$ values concomitant with higher $\delta^{18}O_{Cw}$ (see Supplementary materials); among them, three were dated at approximately 42–43 kyr BP and 49–50 kyr BP (i.e. at times when the r^2 shifted towards more positive values during the MIS3 (Fig. 4)). These replicated samples tend to confirm the idea that some r^2 excursions could have occurred on the millennial timescale in synchronicity with Heinrich events. Whether smooth r^2 positive shifts at these times are a real signal for rapid changes in the latitudinal $\delta^{18}O_{sw}$ gradient still needs to be confirmed. However if these r^2 features turn out to be real, they are in line with the theory for increased AAIW formation during Heinrich events that can be potentially linked to increased subduction of surface waters through surface water density increases (Schulte et al., 1999; Pahnke and Zahn, 2005; Schmittner, 2005; Schmittner et al., 2007; Schmittner and Galbraith, 2008).

Why the northern nutrient-rich water mass end-member have spread as far as the MD02-2529 core location during most of MIS3, 4, and 5 is hard to understand. As previously discussed, one possibility could be the sustained formation of GNPIW during these times that eventually reaches the Panama Basin from time to time when waters from a southern origin did not reach the northern hemisphere. During these times, the r^2 likely indicates that northern end-member waters may have been of a higher density than those of southern origin. Another possibility is that the northern origin of nutrient-rich waters spreading in the Panama Basin would be a part of the return pathway of deep and bottom waters that may have originated from the Southern Ocean, as for the mechanism described in Lund and Mix (1998) that explains rapid changes in ventilation "from below." Such a hypothesis may explain how $\delta^{13}C_{Cw}$ can acquire such negative values, and is one reason for the high $\delta^{18}O_{Cw}$ acquired upstream in the Southern Ocean, where the highest density and $\delta^{18}O_{sw}$ of the world ocean were found for the LGM (Adkins et al., 2002).

7. Conclusions

We measured stable isotopes on benthic foraminifera from the MD02-2529 marine sediment core collected in Panama Basin at ~1600 m water depth, which spans the last 150 kyr BP. The $\delta^{13}C_{Cw}$ record is characterized by relatively stable and high values for the last 25 kyr BP, as compared to earlier time periods when $\delta^{13}C_{Cw}$ values were more variable at millennial and longer timescales. We found that millennial-scale $\delta^{13}C_{Cw}$ anomalies prior to 25 kyr BP were negatively correlated with millennial-scale $\delta^{18}O_{Cw}$ anomalies. We interpret this feature as reflective of rapid movements of a water mass front separating two water masses with distinct geochemical and $\delta^{18}O_{sw}$ and/or temperature characteristics.

$\delta^{13}C_{Cw}$ shifts at millennial and longer timescales can attain 1‰ and roughly correspond to the $\delta^{13}C$ gradient found between two water masses located further north and south within the same depth range. Therefore, the MD02-2529 $\delta^{13}C_{Cw}$ record reflects water mass advection from two remote end-members localized northward and southward that alternately bathed the coring site.

The MD02-2529 $\delta^{13}C_{Cw}$ record indicates that mid-depth waters from northern sources intermittently spread as far as 8°N prior to 25 kyr BP, and competed with waters of a southern origin. The millennial-scale covariation between the $\delta^{13}C_{Cw}$ and the $\delta^{18}O_{Cw}$ records indicates that the northern water mass was saltier (or colder) than the southern water mass during most of the last glacial period. This result suggests that most of the last glacial period was marked by enhanced circulation originating from the North Pacific.

Depending on whether or not the latitudinal gradient in water temperature and/or salinity that we identified reflects the water mass properties of GNPIW or of the deeper waters remotely connected to the Southern Ocean is premature. Nonetheless, the record provides new important benchmarks for paleomodelling experiments in which temperature and salinity fields can be compared to past changes in the Pacific meridional overturning circulation under glacial boundary conditions.

Supplementary materials related to this article can be found online at doi:10.1016/j.epsl.2010.08.002.

Acknowledgements

We thank Frauke Rostek for measuring alkenones and Corinne Sonzogni for performing the stable isotope analyses. We thank Jess Adkins, Alan Mix, Olivier Marchal, Rainer Zahn, and Cécile Blanchet for the discussions and advices. We thank Yiming Wang for the English language editing. The quality of the manuscript was substantially

improved by the constructive comments of Peter deMenocal and two anonymous reviewers.

References

Adkins, J.F., McIntyre, K., Schrag, D.P., 2002. The salinity, temperature and $\delta^{18}O$ content of the glacial deep ocean. Science 298, 1769–1773.

Adkins, J.F., Boyle, E.A., Curry, W.B., 2003. Stable isotopes in deep-sea corals and a new mechanism for "vital effects". Geochim. Cosmochim. Acta 67, 1129–1143.

Bard, E., Rostek, F., Ménot-Combes, G., 2004. Radiocarbon calibration beyond 20,000 14C yr B.P. by means of planktonic foraminifera of the Iberian Margin. Quater. Res. 61, 204–214.

Behl, R.J., Kennett, J.P., 1996. Brief interstadial events in the Santa Barbara basin, NE Pacific, during the last 60 kyr. Nature 379, 243–246.

Blanchet, C., Thouveny, N., Vidal, L., Leduc, G., Tachikawa, K., Bard, E., Beaufort, L., 2007. Terrigenous input response to glacial/interglacial climatic variations over South Baja California: a rock magnetic approach. Quatern. Sci. Rev. 26, 3118–3133.

Blanchet, C.L., Thouveny, N., Vidal, L., 2009. Formation and preservation of greigite (Fe_3S_4) in sediments from the Santa Barbara Basin: implications for paleoenvironmental changes during the past 35 ka. Paleoceanography 24, PA2224. doi:10.1029/2008PA001719.

Blunier, T., Brook, E.J., 2001. Timing of millennial-scale climate change in Antarctica and Greenland during the last glacial period. Science 291, 109–112.

Charles, C.D., Pahnke, K., Zahn, R., Mortyn, P.G., Ninnemann, U., Hodell, D.A., 2010. Millennial scale evolution of the Southern Ocean chemical divide. Quatern. Sci. Rev. 29, 399–409.

Conkright, M.E., Boyer, T.P., 2002. World Ocean Atlas 2001: Objective Analyses, Data statistics, and Figures, CD-ROM Documentation. National Oceanographic Data Center, Silver Spring, MD. 17 pp.

Craig, H., Gordon, L.I., 1965. Deuterium and oxygen-18 variations in the ocean and the marine atmosphere. In: Tongiorgi, E. (Ed.), Proceedings of a Conference on Stable Isotopes in Oceanographic Studies and Paleotemperatures. Spoleto, Italy, pp. 9–130.

Delaygue, G., Jouzel, J., Dutay, J.C., 2000. Oxygen 18–salinity relationship simulated by an oceanic general circulation model. Earth Planet. Sci. Lett. 178, 113–123.

Duplessy, J.C., Shackleton, N.J., Matthews, R.B., Prell, W., Ruddiman, W.F., Caralp, M., Hendy, C.H., 1984. ^{13}C record of benthic foraminifera in the last interglacial ocean: implications for the carbon cycle and the global deep water circulation. Quatern. Res. 21, 225–243.

Duplessy, J.-C., Shackleton, N.J., Fairbanks, R.G., Labeyrie, L., Oppo, D., Kallel, N., 1988. Deep water source variations during the last climatic cycle and their impact on the global deep water circulation. Paleoceanography 3, 343–360.

Emile-Geay, J., Madec, G., 2009. Geothermal heating, diapycnal mixing and the abyssal circulation. Ocean Sci. Discuss. 5, 281–325.

Emile-Geay, J., Cane, M.A., Naik, N., Seager, R., Clement, A.C., van Geen, A., 2003. Warren revisited: atmospheric freshwater fluxes and "Why is no deep water formed in the North Pacific". J. Geophys. Res. 108. doi:10.1029/2001JC001058.

Fiedler, P.C., Talley, L.D., 2006. Hydrography of the eastern tropical Pacific: a review. Prog. Oceanogr. 69, 143–180.

Ganopolski, A., Roche, D.M., 2009. On the nature of lead–lag relationships during glacial–interglacial climate transitions. Quatern. Sci. Rev. 28, 3361–3378.

Gorbarenko, S.A., Harada, N., Malakhov, M.I., Vasilenko, Y.P., Bosin, A.A., Goldberg, E.L., 2010. Orbital and millennial-scale environmental and sedimentological changes in the Okhotsk Sea during the last 350 kyr, Global Planet. Change 72, 79–85.

Gu, D., Philander, S.G.H., 1997. Interdecadal climate fluctuations that depend on exchanges between the tropics and extratropics. Science 275, 805–807.

Haug, G.H., Sigman, D.M., 2009. Polar twins. Nat. Geosci. 2, 91–92.

Helly, J.J., Levin, L.A., 2004. Global distribution of naturally occurring marine hypoxia on continental margins. Deep Sea Res. I 51, 1159–1168.

Hendy, I.L., Kennett, J.P., 2003. Tropical forcing of North Pacific intermediate water distribution during Late Quaternary rapid climate change? Quatern. Sci. Rev. 22, 673–689.

Herguera, J.C., Jansen, E., Berger, W.H., 1992. Evidence for a bathyal front at 2000-M depth in the glacial Pacific, based on a depth transect on Ontong Java Plateau. Paleoceanography 7, 3. doi:10.1029/92PA00869.

Herguera, J.C., Herbert, T., Kashgarian, M., Charles, C., 2010. Intermediate and deep water mass distribution in the Pacific during the Last Glacial Maximum inferred from oxygen and carbon stable isotopes. Quater. Sci. Rev. 29, 1228-1245.

Horikawa, K., Asahara, Y., Yamamoto, K., Okazaki, Y., 2010. Intermediate water formation in the Bering Sea during glacial periods: evidence from neodymium isotope ratios. Geology 38, 435–438.

Hughen, K.A., et al., 2004. MARINE04 marine radiocarbon age calibration, 0–26 ka BP. Radiocarbon 46, 1059–1086.

Jorissen, F.J., 1999. Benthic foraminiferal microhabitats below the sediment–water interface. In: Sen Gupta, B.K. (Ed.), Modern Foraminifera. Kluwer Academic Publishers, Great Britain, pp. 161–179.

Jung, S.J.A., Kroon, D., Ganssen, G., Peeters, F., Ganeshram, R., 2009. Enhanced Arabian Sea intermediate water flow during glacial North Atlantic cold phases. Earth Planet. Sci. Lett. 280, 220–228.

Keigwin, L.D., 1987. North Pacific deep water formation during the latest glaciations. Nature 330, 362–364.

Keigwin, L.D., 1998. Glacial-age hydrography of the far northwest Pacific Ocean. Paleoceanography 13, 323–339.

Kennett, J.P., Ingram, B.L., 1995. A 20,000-year record of ocean circulation and climate change from the Santa Barbara basin. Nature 377, 510–514.

Kroopnick, P.M., 1985. The distribution of ^{13}C and ΣCO_2 in the world oceans. Deep-Sea Res. 32, 57–84.

Kuhlbrodt, T., Griesel, A., Montoya, M., Levermann, A., Hofmann, A., Rahmstorf, S., 2007. On the driving processes of the Atlantic meridional overturning circulation. Rev. Geophys. 45. doi:10.1029/2004RG000166.

Leduc, G., Vidal, L., Tachikawa, K., Rostek, F., Sonzogni, C., Beaufort, L., Bard, E., 2007. Moisture transport across Central America as a positive feedback on abrupt climatic changes. Nature 445, 908–911.

Leduc, G., Vidal, L., Cartapanis, O., Bard, E., 2009. Modes of eastern equatorial Pacific thermocline variability: implications for ENSO dynamics over the last glacial period. Paleoceanography 24, 3. doi:10.1029/2008PA001701.

Lisiecki, L.E., Raymo, M.E., 2005. A Pliocene–Pleistocene stack of 57 globally distributed benthic $\delta^{18}O$ records. Paleoceanography 20. doi:10.1029/2004PA001071.

Lund, D., Mix, A., 1998. Millennial-scale deep water oscillations: reflections of the North Atlantic in the Deep Pacific from 10 to 60 ka. Paleoceanography 13 (1), 10–19.

Lynch-Stieglitz, J., Fairbanks, R.G., 1994. A conservative tracer for glacial ocean circulation from carbon isotope and palaeo-nutrient measurements in benthic foraminifera. Nature 369, 308–310.

Lynch-Stieglitz, J., Curry, W.B., Slowey, N., 1999. A geostrophic transport estimate for the Florida Current from the oxygen isotope composition of benthic foraminifera. Paleoceanography 14, 360–373.

Mackensen, A., Hubberten, H.-W., Bickert, T., Fischer, G., Fütterer, D.K., 1993. The $\delta^{13}C$ in benthic foraminiferal tests of Fontobia wuellerstorfi (Schwager) relative to the $\delta^{13}C$ of dissolved inorganic carbon: implications for glacial ocean circulation models. Paleoceanography 8, 587–610.

Matsumoto, K., 2007. Radiocarbon-based circulation age of the world oceans. J. Geophys. Res. 112, C09004. doi:10.1029/2007JC004095.

Matsumoto, K., Oba, T., Lynch-Stiegltiz, J., Yamamoto, H., 2002. Interior hydrography and circulation of the glacial Pacific Ocean. Quatern. Sci. Rev. 21, 1693–1704.

McCave, I.N., Carter, L., Hall, I.L., 2008. Glacial–interglacial changes in water mass structure and flow in the SW Pacific Ocean. Quartern. Sci. Rev. 27, 1886–1908.

McCorkle, D.C., Emerson, S.R., Quay, P.D., 1985. Stable carbon isotopes in marine porewaters. Earth Planet. Sci. Lett. 74, 13–26.

Mikolajewicz, U., Crowley, T.J., Schiller, A., Voss, R., 1997. Modelling teleconnections between the North Atlantic and North Pacific during the Younger Dryas. Nature 387, 384–387.

Mix, A.C., Pisias, N.G., Zahn, R., Rugh, W., Lopez, C., Nelson, K., 1991. Carbon-13 in Pacific deep and intermediate waters, 0–370 ka: implications for ocean circulation and Pleistocene CO_2. Paleoceanography 6, 205–226.

Mix, A.C., Lund, D.C., Pisias, N.G., Bodén, P., Bornmalm, L., Lyle, M., Pike, J., 1999. Rapid climate oscillations in the Northeast Pacific during the last deglaciation reflect northern and southern hemisphere sources. In: Clark, P.U., Webb, R.S., Keigwin, L.D. (Eds.), Mechanisms of Global Climate Change at Millennial Time Scales. AGU Monograph, 112. American Geophysical Union, Washington DC, pp. 127–148.

Ninnemann, U.S., Charles, C.D., 2002. Changes in the mode of Southern Ocean circulation over the last glacial cycle revealed by foraminiferal stable isotopic variability. Earth Planet. Sci. Lett. 201, 383–396.

Okazaki, Y., Timmermann, A., Menviel, L., Harada, N., Abe-Ouchi, A., Chikamoto, M.O., Mouchet, A., Asahi, H., 2010. Deepwater formation in the North Pacific during the last glacial termination. Science 329, 200–204.

Ortiz, J.D., O'Connell, S.B., DelViscio, J., Dean, W.E., Carriquiry, J.D., Marchitto, T., Zheng, Y., van Geen, A., 2004. Enhanced marine productivity off western North America during warm climate intervals of the past 52 k.y. Geology 32, 521–524.

Pahnke, K., Zahn, R., 2005. Southern hemisphere watermass conversion linked with North Atlantic climate variability. Science 307, 1741–1746.

Pailler, D., Bard, E., 2002. High frequency paleoceanographic changes during the past 140 000 yr recorded by the organic matter in sediments of the Iberian Margin. Palaeogeogr. Palaeclim. Palaeoecol. 181, 431–452.

Pearson, P., Ditchfield, P.W., Singano, J., Harcourt-Brown, K.G., Nicholas, C.J., Olsson, R.K., Shackleton, N.J., Hall, M.A., 2001. Warm tropical sea surface temperature in the Late Cretaceous and Eocene epochs. Nature 413, 481–487.

Pena, L.D., Cacho, I., Ferretti, P., Hall, M.A., 2008. El Niño–Southern oscillation-like variability during glacial terminations and interlatitudinal teleconnections. Paleoceanography 23, 3. doi:10.1029/2008PA001620.

Pichevin, L., Bard, E., Martinez, P., Billy, I., 2007. Evidence of ventilation changes in the Arabian Sea during the late Quaternary: implication for denitrification and nitrous oxide emission. Glob. Biogeochem. Cycles 21, GB4008. doi:10.1029/2006GB002852.

Reid, J.L., 1997. On the total geostrophic circulation of the pacific ocean: flow patterns, tracers, and transports. Prog. Oceanog. 39, 263–352.

Saenko, O.A., Schmittner, A., Weaver, A.J., 2004. The Atlantic–Pacific seesaw. J. Climate 17, 2033–2038.

Schmittner, A., 2005. Decline of the marine ecosystem caused by a reduction in the Atlantic overturning circulation. Nature 434, 628–633.

Schmittner, A., Galbraith, E.D., 2008. Glacial greenhouse gas fluctuations controlled by ocean circulation changes. Nature 456, 373–376.

Schmittner, A., Galbraith, E.D., Hostetler, S.W., Pedersen, T.F., Zhang, R., 2007. Large fluctuations of dissolved oxygen in the Indian and Pacific oceans during Dansgaard–Oeschger oscillations caused by variations of North Atlantic Deep Water subduction. Paleoceanography 22, PA3207. doi:10.1029/2006PA001384.

Schulte, S., Rostek, F., Bard, E., Rullkötter, J., Marchal, O., 1999. Variations of oxygen-minimum and primary productivity recorded in the sediments of the Arabian Sea. Earth Planet. Sci. Lett. 173, 207–221.

Shackleton, N.J., 1977. Carbon-13 in Uvigerina: tropical rainforest history and the equatorial pacific carbonate dissolution cycles. In: Andersen, N.R., Malahoff, A. (Eds.), The Fate of Fossil Fuel CO_2 in the Oceans. New York.

Siddall, M., Rohling, E.J., Thompson, W.G., Waelbroeck, C., 2008. Marine isotope stage 3 sea level fluctuations: data synthesis and new outlook. Rev. Geophys. 46, RG4003. doi:10.1029/2007RG000226.

Sigman, D.M., Hain, M.P., Haug, G.H., 2010. The polar ocean and glacial cycles in atmospheric CO_2 concentration. Nature 466, 47–55.

Sonzogni, C., Bard, E., Rostek, F., Dollfus, D., Rosell-Mélé, A., Eglington, G., 1997. Temperature and salinity effects on alkenone ratios measured in surface sediments from the Indian Ocean. Quatern. Res. 47, 344–355.

Spero, H.J., Bijma, J., Lea, D.W., Bemis, B.E., 1997. Effect of seawater carbonate concentration on foraminiferal carbon and oxygen isotopes. Nature 390, 497–500.

Spero, H.J., Mielke, K.M., Kalve, E.M., Lea, D.W., Pak, D.K., 2003. Multispecies approach to reconstructing eastern equatorial Pacific thermocline hydrography during the past 360 kyr. Paleoceanography 18. doi:10.1029/2002PA000814.

Stott, L.D., Neumann, M., Hammond, D., 2000a. Intermediate water ventilation on the Northeastern Pacific margin during the late Pleistocene inferred from benthic foraminiferal $\delta^{13}C$. Paleoceanography 15, 161–169.

Stott, L.D., Berelson, W., Douglas, R., Gorsline, D., 2000b. Increased dissolved oxygen in Pacific intermediate waters due to lower rates of carbon oxidation in sediments. Nature 407, 367–370.

Stuiver, M., Grootes, P.M., 2000. GISP2 oxygen isotope ratios. Quatern. Res. 53, 277–284.

Talley, L.D., 1993. Distribution and formation of North Pacific Intermediate Water. J. Phys. Oceanogr. 23, 517–537.

Torres, M.E., Mix, A.C., Kinports, K., Haley, B., Klinkhammer, G.P., McManus, J., de Angelis, M.A.A., 2003. Is methane venting at the seafloor recorded by $\delta^{13}C$ of benthic foraminifera shells? Paleoceanography 18. doi:10.1029/2002PA000824.

Tsuchiya, M., Talley, L.D., 1996. Water-property distributions along an eastern Pacific hydrographic section at 135 W. J. Mar. Res. 54, 541–564.

van Geen, A., Fairbanks, R.G., Dartnell, P., McGann, M., Gardner, J.V., Kashgarian, M., 1996. Ventilation changes in the northeast Pacific during the last deglaciation. Paleoceanography 11, 519–528.

van Geen, A., Zheng, Y., Bernhard, J.M., Cannariato, K.G., Carriquiry, J., Dean, W.E., Eakins, B.W., Ortiz, J.D., Pike, J., 2003. On the preservation of laminated sediments along the western margin of North America. Paleoceanography 18, 1098. doi:10.1029/2003PA000911.

VanLaningham, S., Pisias, N.G., Duncan, R.A., Clift, P.D., 2009. Glacial–interglacial sediment transport to the Meiji Drift, northwest Pacific Ocean: evidence for timing of Beringian outwashing. Earth Planet. Sci. Lett. 277, 64–72.

Vidal, L., Labeyrie, L., Cortijo, E., Arnold, M., Duplessy, J.C., Michel, E., Becqué, S., van Weering, T.C.E., 1997. Evidence for changes in the North Atlantic deep water linked to meltwater surges during the Heinrich events. Earth Planet. Sci. Lett. 146, 13–27.

Warren, B.A., 1983. Why is no deep water formed in the North Pacific? J. Mar. Res. 41, 327–347.

Wu, G., Berger, W., 1989. Planktonic foraminifera: differential dissolution and the quaternary stable isotope record in the west equatorial Pacific. Paleoceanography 4, 181–198.

Wunsch, C., 2003. Determining paleoceanographic circulations, with emphasis on the Last Glacial Maximum. Quatern. Sci. Rev. 22, 371–385.

Zahn, R., Pedersen, T.F., Bornhold, B.D., Mix, A.C., 1991. Water mass conversion in the glacial subarctic Pacific (54°N, 148°W): physical constraints and the benthic-planktonic stable isotope record. Paleoceanography 6, 5. doi:10.1029/91PA01327.